Neurochemistry International 126 (2019) 86–95

Contents lists available at ScienceDirect

Neurochemistry International

journal homepage: www.elsevier.com/locate/neuint

Therapeutic hypothermia protects photoreceptors through activating Cirbp pathway

Ying-Jian Sun[a], Sen Ma[a], Bin Fan[a], Ying Wang[b], Shu-Rong Wang[a], Guang-Yu Li[a,*]

[a] Department of Ophthalmology, Second Hospital of Jilin University, Changchun, PR China
[b] Department of Hemooncology, Second Hospital of Jilin University, Changchun, PR China

ARTICLE INFO

Keywords:
Hypothermia
Photoreceptors
Cold-inducible RNA-Binding protein
Retina
Glucose deprivation
Apoptosis

ABSTRACT

Therapeutic hypothermia as a physical method to lower the brain temperature of patients has been widely used in clinics as an effective and necessary step during the treatment of acute brain injury or edema. However, due to limitations of the ocular structure, the application of hypothermia in retinal neuroprotection still has an obvious barrier. Here, the neuroprotective mechanism produced by hypothermia in the retina was investigated, with the hopes of deciphering the key molecular targets of the signaling pathway to finally realize the ocular neuroprotection by regulating specific molecular targets. In present study, it was first demonstrated that hypothermia produced significant neuroprotection on photoreceptors (661 W cell) against glucose deprivation (GD)-induced injury *in vitro* and visible light-induced retinal damage *in vivo*. The results disclosed that hypothermia (32 °C) was able to attenuate the upregulation of heme oxygenase-1, cleaved Caspase-3, cleaved Caspase-9, and B-cell lymphoma-2-associated X caused by GD, and restored the decline of protective factor B-cell lymphoma-2 as well. Moreover, hypothermia suppressed the excessive generation of intracellular reactive oxygen species and depolarization of mitochondrial membrane potential, and showed marked neuroprotection against GD-induced damage in photoreceptors, which significantly reduced cell death percentage *in vitro*. In *in vivo* experiments, it was found that hypothermia was able to protect retinal function against light injury, restoring the decline of a-waves and b-waves in electroretinograms and maintaining the thickness of the retinal outer nuclear layer. Furthermore, hypothermia blocked the visible light-induced cell death pathway in the retina, suppressing poly(ADP-ribose) polymerase-1 activation. More importantly, it was demonstrated that cold-inducible RNA-binding protein (Cirbp) as a key molecular target played an important role in hypothermia-induced neuroprotection, which is the first proof of its function in ophthalmology. In *in vitro* experiments, hypothermia caused marked expression of Cirbp in photoreceptors. And reducing the expression of Cirbp with specific small interfering RNA was able to block the hypothermia-induced neuroprotection. Consistently, overexpressed Cirbp with Cirbp-gene-modified lentivirus mimicked the neuroprotection against GD-induced injury even under normal temperature (37 °C) conditions. Additionally, the overexpression of Cirbp was detected in hypothermia-treated retinas. These results indicate that hypothermia promotes neuroprotection in photoreceptors via activation of the Cirbp pathway. The study presented here suggests that therapeutic hypothermia may promote neuroprotection in the retina by activating Cirbp, and regulating Cirbp may mimic similar protection even under normal temperature conditions, which might be a specific molecular target in retinal neuroprotection.

1. Introduction

Therapeutic or protective hypothermia, normally through a physical and/or medical means to maintain a specific body temperature in a patient for a certain duration of time, improves health outcomes during the treatment of acute brain injury. Plenty of clinical studies have demonstrated that therapeutic hypothermia has neuroprotective effects on comatose patients with spontaneous circulation after out-of-hospital cardiac arrest (Dell'Anna et al., 2014; Demirgan et al., 2014; Dzieciol et al., 2014). In animal models, therapeutic hypothermia also provided protection in hippocampal neurons caused by oxygen-glucose deprivation/reperfusion injury (Zhou et al., 2017), or against acute ischemia-induced brain injury in sheep (Cattaneo et al., 2016). In addition, hypothermia also has been found to provide a protective effect on retinas against light damage and ischemic injury (Mori et al., 1997; Reinhard et al., 2016; Salido et al., 2013).

* Corresponding author.
E-mail address: liguangyu@aliyun.com (G.-Y. Li).

https://doi.org/10.1016/j.neuint.2019.03.006
Received 21 November 2018; Received in revised form 14 February 2019; Accepted 6 March 2019
Available online 14 March 2019
0197-0186/

Previous studies have demonstrated that extracellular calcium-sensing receptors can be activated during hypothermia (Kim et al., 2013) and mitochondrial apoptosis can be blocked by hypothermic treatment (Wu et al., 2017). However, the exact mechanism of hypothermia-induced neuroprotection is still unclear. Recently, some evidence shows that cold-inducible RNA-binding protein (Cirbp) plays an important role in the anti-apoptotic effect of hypothermia (Li et al., 2012; Wu et al., 2017; Zhang et al., 2015). Cirbp has an RNA-binding factor composed of an N-terminal RNA Recognition Motif (RRM) and a C-terminal region containing several repeats of the arginine-glycine-rich (RGG) motif (Zhu et al., 2016). Under hypothermia conditions, the upregulation of Cirbp expression enhanced the translation of specific mRNAs by binding to the 5′-untranslated region (UTR) or 3′-UTR of different transcripts (Sahara et al., 2002). Iftode et al. demonstrated that Cirbp was able to specifically bind to the 3′-UTR of thioredoxin (TRX) (Iftode et al., 1999), and TRX may protect oxidative stress-injured cells by quenching reactive oxygen species (ROS) (Xu et al., 2006). Additionally, overexpressing Cirbp blocked caspase-dependent apoptosis in cortical neurons by activating B-cell lymphoma-2 (Bcl-2) and suppressing Bcl-2-associated X (BAX) (Li et al., 2012).

Retina ischemia and light injury have been considered as important factors in the pathogenesis of retinal degeneration (Chao et al., 2014; Osborne et al., 2004; Peng et al., 2011; Wenzel et al., 2005). For retinal ischemia, decreased glucose levels resulting in acute energy failure contribute to the death of photoreceptors and subsequent vision injury, since over 80% of glucose uptake by photoreceptors is used for anaerobic glycolysis, producing more than 50% of total adenosine triphosphate when O_2 is available (Winkler, 1981). Fan et al. revealed acute energy depletion or glucose deprivation induced oxidative stress injury and a caspase-dependent death in photoreceptors (661w cell) (Fan et al., 2017). However, light-induced death in photoreceptor cells is mediated by a caspase-independent mechanism called parthanatos. Parthanatos does not require caspases but is dependent on the overactivation of poly(ADP-ribose) polymerase-1 (PARP-1). Liu et al. showed the level of PARP-1 and the apoptosis-inducing factor (AIF) were upregulated following light exposure. PARP-1 knockdown significantly decreased light exposure-induced cell apoptosis and proved that light-induced death is via PARP-1 dependent pathway (Liu et al., 2018).

In the present study, acute energy depletion was mimicked using glucose deprivation (GD), and the protective effect and mechanism of hypothermia on GD-induced injury in photoreceptors (661 W cell) were mainly investigated and the role of Cirbp as an important factor in regulating hypothermic protection was further demonstrated. In addition, the neuroprotection of hypothermia on retina against light-induced damage with a mice model was also verified *in vivo*.

2. Materials and methods

2.1. Cell culture

A photoreceptor cell (661 W cell) line was generously provided by Dr. Muayyad Al-Ubaidi (University of Oklahoma Health Sciences Center, Oklahoma, USA). Cells were grown in Dulbecco's modified Eagle's medium (Hyclone Laboratories, Inc. Logan, Utah, USA) supplemented with 10% heat-inactivated fetal calf serum (Hyclone) and 2% penicillin/streptomycin (Hyclone), at 37 °C in a humidified atmosphere with 5% carbon dioxide. For glucose deprivation (GD) experiments, 661 W cells were cultured in 96- or 24-well plates for 24 h, collected from medium, washed three times with phosphate-buffered saline (PBS), and then cultured in glucose-free medium at indicated time points. There were four groups in the *in vitro* experiments: 1. Con37, a control group of 661 W cells cultured in growth medium with glucose at 37 °C; 2. GD37, 661 W cells cultured in glucose-free medium at 37 °C; 3. Con32, a control group of 661 W cells cultured in growth medium with glucose at 32 °C; 4. GD32, 661 W cells cultured in glucose-free medium at 32 °C.

2.2. MTT assay

The 661 W cells were seeded at 1×10^4 cells per well in 96-well plates. Ten microliters of (3-(4,5-dimethyl-2-thiazolyl)-2,5-diphenyltetrazolium bromide (MTT), 5 mg/ml, Sigma-Aldrich, St. Louis, MO, USA) was added to each well at a final concentration of 500 μg/ml and incubated for 1 h at 37 °C. Following incubation, supernatant was removed, and 100 μL dimethyl sulfoxide (DMSO) was added to each well, followed by incubation at 37 °C overnight. Absorbance was measured at 570/650 nm using an Infinite M200 promicroplate reader (Tecan, Mannedorf, Switzerland).

2.3. Propidium Iodide (PI)/Hoechst staining

Cells from different groups were stained in the dark with staining solution (2 μg/ml of PI/Hoechst, Beyotime Biotechnology, Shanghai, China) for 10 min at room temperature. PI-positive cells were visualized under an inverted fluorescence microscope (Olympus, Tokyo, Japan). Quantitative assessment of cell death was performed with flow cytometry.

2.4. Annexin V-Fluorescein isothiocyanate (FITC)/PI assay

Cells were collected from each group, washed twice with cold PBS (4 °C), resuspended in 200 μL staining buffer at 1×10^6 cells/mL plus 10 μL of Annexin V- fluorescein isothiocyanate (FITC) (Sungene Biotech, Tianjin, China) with gentle mixing, incubated in the dark at room temperature for 15 min, supplemented with an additional 300 μL of staining buffer with 7.5 μL of PI solution (20 μg/ml) and incubated at room temperature for 5 min. Apoptotic cells were detected by flow cytometry (ACEA Biosciences, Inc, Hangzhou, China).

2.5. Intracellular reactive oxygen species (ROS) measurement

Intracellular ROS was measured with an oxidation-sensitive fluorescence probe 2′,7' dichlorodihydrofluorescin diacetate (DCFH-DA, Beyotime Biotechnology, Shanghai, China) and dihydroethidium (DHE, Beyotime Biotechnology, Shanghai, China). For ROS measurement, photoreceptors (661 W cells) were cultured in 6-well plates with growth medium or glucose-free medium for 16 h, washed twice with fresh medium, then incubated in 10 μM DCFH-DA or DHE at 37 °C for 20 min. The fluorescence was visualized under a fluorescence microscope (Olympus, Tokyo, Japan). Fluorescence intensities were quantitatively analyzed using Image J software v1.44 (NIH, Bethesda, MD, US).

2.6. Mitochondrial-membrane potential assay ($\Delta\psi m$)

Medium from each group was removed, and cells were washed with Ca^{2+}/Mg^{2+}-free PBS, stained with 5,5′,6,6′-Tetrachloro-1,1′,3,3′-tetraethylbenzimidazolo-carbocyanine iodide (10 μg/ml, Beyotime Biotechnology, Shanghai, China), incubated at 37 °C for 30 min, washed with JC-1 staining buffer twice, and then examined under an inverted fluorescence microscope (Olympus). Normal cells are indicated by red fluorescence at normal mitochondrial membrane potential. Meanwhile, apoptotic cells are indicated by green fluorescence because mitochondrial membrane potential collapses.

2.7. Assays of overexpression or expression inhibition of cold-inducible RNA-Binding protein (Cirbp)

A lentiviral vector encoded with Cirbp (GeneCopoeia, Rockville, MD, US), and a lentiviral vector (Lenti-XTM) encoded with Cirbp shRNA (5′- GGGTCCTACAGAGACAGCTATGACATTCAAGAGATGTCATAGCTGTCTCTGTAGGACCC-3) (Takara Bio Clontech, Mountain View,

CA, US) were amplified using a Lenti-Pac™HIV Expression Packaging Kit (GeneCopoeia). Lentiviruses were titrated in 293T cells, and their titers were 1×10^8 TU/ml. The 661 W cells were transduced by Lenti-Cirbp or Lenti-shCirbp at 100 TU/cell. Lenti-green fluorescent protein was used as a control vector (GeneCopoeia, Rockville, MD, US).

2.8. Western blot analysis

For western blot analysis, 661 W cells from each group were sonicated in protein lysate buffer to extract whole cell protein, and protein concentrations were measured using the bicinchoninic acid assay. Twenty micrograms of protein from each sample was used for western blot analysis in a 10% polyacrylamide gel containing 0.1% sodium dodecyl sulfate, followed by transfer to nitrocellulose membranes. Primary antibodies used for western blotting were rabbit polyclonal anti-activating B-cell lymphoma-2 (Bcl-2) antibody (1:1000 dilution, Beyotime Biotechnology, Shanghai, China), rabbit polyclonal anti-Bcl-2-associated X antibody (1:1000 dilution, Beyotime Biotechnology, Shanghai, China), rabbit polyclonal anti-Caspase-3 antibody (1:1000 dilution, Cell Signaling Technology, Danvers, MA, USA), rabbit polyclonal anti-Caspase-9 antibody (1:1000 dilution, Cell Signaling Technology, Danvers, MA, USA), rabbit polyclonal anti-heme oxygenase-1 antibody (1:1000 dilution, Bioworld Technology, Minneapolis, MN, US), rabbit polyclonal anti-Cirbp antibody (1:500 dilution, Proteintech, Wuhan, China), mouse polyclonal anti-β-actin antibody (1:1000 dilution, Signalway Technology, St. Louis, MO, US), and rabbit polyclonal anti-poly(ADP-ribose) polymerase-1 antibody (1:2500 dilution, Cell Signaling Technology, Danvers, MA, USA). Rabbit polyclonal biotinylated secondary (1:3000 dilution, Signalway Technology, St. Louis, MO, US) was used to detect positive signals using enhanced chemiluminescence (Millipore, Billerica, MA, U.S.A), and images were captured using a microscope equipped with a charge coupled device (CCD) camera (Tanon, Shanghai, China).

2.9. Animal

The animal experimental protocol was approved by the Institutional Animal Care, Use Committee and the Ethics Committee of the Second Hospital of Jilin University, Changchun, China (approval number: 2018038). Twenty male six-week-old C57BL/6 J mice were obtained from Liaoning Changsheng Biotechnology (Catalog No. 211002300026556) and kept in a temperature-controlled room (22 ± 1 °C) with relative humidity maintained between 30% and 70% and a 12-h light:12-h dark cycle.

2.10. Light exposure and hypothermic assay

Light exposure was performed as described (Wang et al., 2012). Briefly, animals were kept in dark for 12 h before experimental light exposure. All of the preparatory steps prior to light exposure were performed under dim red light. First, atropine was dropped in the animals' eyes, and then mice were put into a specially fabricated light box with a white electric bulb (32w, F32T8/TL84, Philips Long Life Plus) under 7500 lux exposure. The lux level was measured inside the box at mouse eye level. After light exposure, mice were returned to a dimly lit cyclic room (5–10 lux) to recover for 5 days. Retinal damage/protection was assessed by functional analysis using an electroretinogram (ERG) and histological morphology analysis by hematoxylin-eosin (HE) staining.

For the light-induced cell experiment, approximately 70% confluent 661 W cells and 661 W cells transduced by Lenti-GFP and Lenti-Cirbp were cultured in 6-well or 96-well plates for 24 h with normal medium at 37 °C. Cells were then cultured in normal medium under light exposure (1500 lx) for the maximum possible duration (until all the cells died) at 37 °C.

For the hypothermic effect assay, there were four groups and five mice for each group. These four groups were randomized by the caretaker in an animal facility. The caretaker was asked to put five mice in each cage randomly, and label cages 1, 2, 3 and 4 upon arrival to the animal facility. Group 1, ConR, was control mice without light exposure at room temperature (24 °C) for 3 days. Group 2, LD was mice with light exposure at room temperature (24 °C) for 3 days. Group 3, ConH, was control mice without light exposure that were kept in a cold room (8 °C) for 3 h each day for 3 days, then on days 4 and 5, mice were kept in a room at room temperature. Group 4, LDH, was mice that were exposed to light and then kept in a cold room (8 °C) for 3 h each day for 3 days, then on days 4 and 5, mice were kept in a room at room temperature (Rey-Funes et al., 2017).

2.11. Electroretinography

Electroretinography (Metrovision, Perenchies, France) was used to evaluate retinal function. The dark-adapted ERG (scotopic 0.01, b-wave) and light-adapted ERG (photopic 3.0, a-wave) were recorded bilaterally after 5 days post-light exposure. Mice were kept in full darkness for 2 h before recording the ERG, then kept in a room with dim red light. Mice were anesthetized intraperitoneally with pentobarbital sodium (60 mg/kg). Both pupils were dilated with 1% tropicamide saline. Proxymetacaine was applied topically for corneal anesthesia, and carbomer was used for treatment of corneal hydration. The temperature of mice was maintained at a body temperature of 36 °C through the use of a heating pad. The ground electrode was a subcutaneous needle in the tail, and the reference electrode was placed subcutaneously under the lower jaw. Active electrodes were sliver wires placed on the cornea. Once the setup was finished, and the dim red light was removed, 10 min of dark adaptation was allowed before commencement of recording. Electroretinographic analysis was based on amplitude measurements of the a- and b-waves. The implicit time of the a- and b-waves was measured from the onset of stimuli to the peak of each wave.

2.12. Morphology observation

The euthanasia of mice from different groups were conducted by injecting anesthesia (80 mg/kg sodium pentobarbital, intraperitoneal), and a marker was made at the 12 o'clock position for each eye using surgical suture needles with thread (Ningbo Medical Needle Co., Ltd, Ningbo, China). All of the collected eyes were immersed in 4% paraformaldehyde for 6 h, washed three times in PBS, then dehydrated in gradient ethanol with xylene and embedded in paraffin, sectioned at 3 μm through the optic disc of each eye, and stained with HE. The thickness of the outer nuclear layer (ONL) was measured at a distance of 0.45–0.55 mm from the optic disc by the straight line tool in the Image J software, because the retinal ONL thickness is a common method to evaluate the effects of light-induced injury. Five sections were selected in every eye to guarantee the accuracy of measuring data.

2.13. Statistical analysis

All experiments were repeated independently 3 times. Data are expressed as means ± standard error of mean (SEM). No statistical methods were used to predetermine sample sizes for the studies, but sample sizes were similar to those generally employed in this field. Data analyses were performed using SPSS statistic software v19.0 (IBM, Armonk, NY, USA). First, we used the Levene's tests to assess homogeneity of variance, which is a precondition for analysis of variance (ANOVA). The results of the tests indicated that variance within each of the populations is equal ($P > 0.05$). Then, differences between means were evaluated using one-way ANOVA with a Bonferroni test. $P < 0.05$ was considered to be statistically significant.

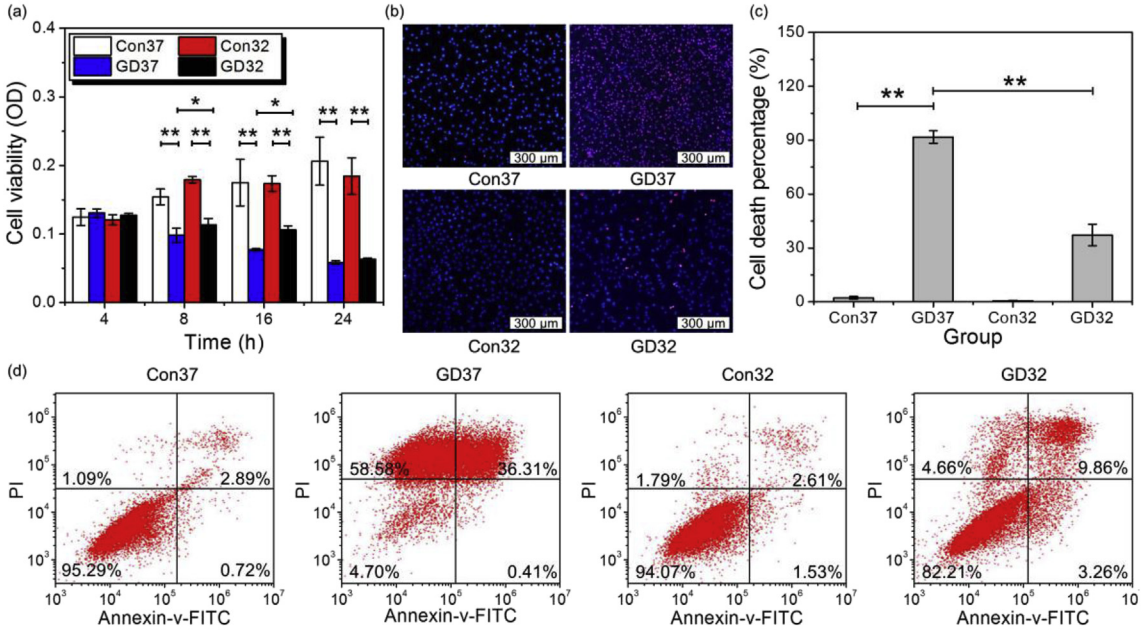

Fig. 1. Hypothermia treatment abrogates GD-injured cell death. (a) The 661 W cells were cultured in glucose-free medium for indicated times at 37 °C or 32 °C by MTT assay. F (8 h) = 82.926. P (Con37, GD37; 8 h) < 0.001. P (Con32, GD32; 8 h) < 0.001. P (GD37, GD32; 8 h) = 0.019. F (16 h) = 36.717. P (Con37, GD37; 16 h) < 0.001. P (Con32, GD32; 16 h) < 0.001. P (GD37, GD32; 16 h) = 0.022. F (24 h) = 63.202. P (Con37, GD37; 16 h) < 0.001. P (Con32, GD32; 16 h) < 0.001. (b) The 661 W cells were cultured in glucose-free medium for 16 h at 37 °C or 32 °C by PI/Hoechst staining. (c) Quantitative assessment of cell death was performed with flow cytometry for PI/Hoechst staining. F = 301.908. P (Con37, GD37) < 0.001. P (GD37, GD32) < 0.001. (d) Data from flow cytometry; 661w cells were stained by Annexin V-FITC and PI staining. Data are shown as means ± SEM. n (number of independent experiments) = 3. ∗: $P < 0.05$, ∗∗: $P < 0.01$.

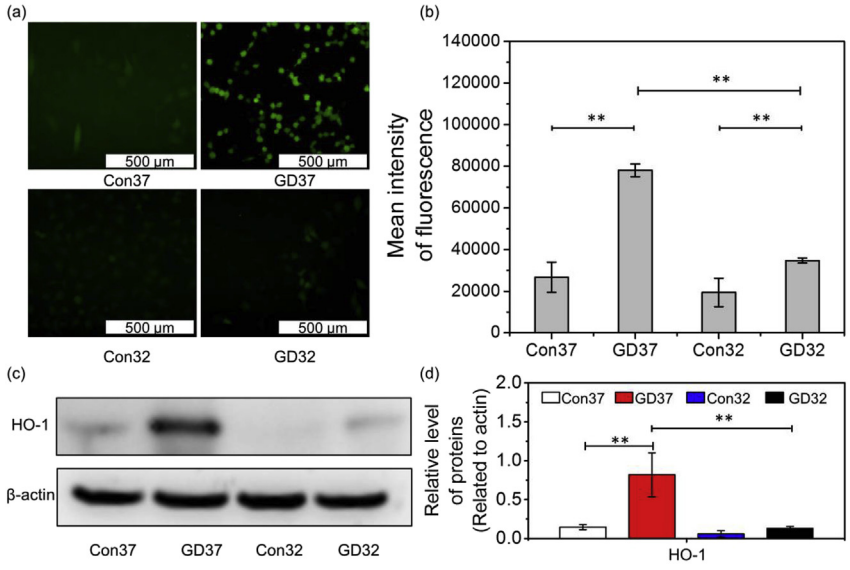

Fig. 2. Hypothermia treatment suppresses GD-induced oxidative stress. (a) Intracellular ROS was measured with DFCH-DA and identified by green fluorescence. (b) Fluorescence intensities were measured and relative fluorescence was statistically analyzed. F = 75.201. P (Con37, GD37) < 0.001. P (Con32, GD32) = 0.007. P (GD37, GD32) < 0.001. (c) HO-1 detected with western blot, β-actin was used as a loading control. The molecular weight of HO-1 and β-actin are 34 and 43 kD, respectively. (d) Protein bands on the western blots were scanned, and the intensity was determined by optical density measurements. F = 12.231. P (Con37, GD37) = 0.002. P (GD37, GD32) = 0.001. These results are presented as means ± SEM. (n (number of independent experiments) = 3. ∗: $P < 0.05$, ∗∗: $P < 0.01$).

3. Results

3.1. Hypothermia protects photoreceptors against GD injury

Three different means were used to assess the neuroprotection produced by hypothermia on GD-injured photoreceptors. As shown in Fig. 1a, 661 W cells were cultured under normal temperature (37 °C) or hypothermia (32 °C). No statistical difference of cell viability was detected between normal and hypothermic cultured groups within 24 h. However, GD caused severe damage in photoreceptors, remarkably reducing the cell viability to 0.0985 ± 0.00982 and 0.1135 ± 0.00891 in both normal and hypothermic cultured groups (F = 82.926. P = 0.019) from 8 h measured with 3-(4,5-dimethyl-2-thiazolyl)-2,5-diphenyltetrazolium bromide (MTT) assay, yet the hypothermia-treated cells were more resistant to the GD injury, showing increased cell viability with statistical significance at 8 and 16 h compared to normal cultured cells. Moreover, the cell death percentages were determined with Propidium Iodide (PI)/Hoechst staining as well. As shown in Fig. 1b, GD treatment led to massive cell death, with PI showing purple-colored fluorescence in dead cells. Consistently, hypothermic treatment markedly delayed cell death, with fluorescence data showing less purpled colored cells. Further quantitative analysis showed that GD treatment caused 90.78 ± 3.44% cell death at 16 h under normal culture conditions, while the hypothermic treatment

reduced cell death percentage significantly to 34.20 ± 5.99% (F = 36.717. P = 0.022). Lastly, the apoptotic rate was evaluated by a PI/Annexin-V-fluorescein isothiocyanate (FITC) assay with flow cytometry. As shown in Fig. 1d, after 16 h of GD treatment, the cell death rate reached about 95%, including 36.72% apoptotic cells at late phase, while the hypothermic treatment reduced the cell death rate from 95.3 to 17.79%, including 13.12% apoptotic cells. These results suggest that hypothermic treatment delays photoreceptors death and protects photoreceptors against GD injury.

3.2. Hypothermia blocks intrinsic caspase-dependent apoptosis pathway

The mitochondria play a key role in intracellular ROS generation and intrinsic apoptotic pathways (Fan et al., 2017). Fig. 2a shows that 16 h GD treatment caused massive ROS generation in photoreceptors, which was indicated by intensive green fluorescence detected with 2′,7′ dichlorodihydrofluorescin diacetate (DCFH-DA) staining, while hypothermia treatment remarkably suppressed the generation of ROS, showing less DCFH-DA stained cells. Quantitative analysis further showed that the mean intensity of fluorescence was reduced from 78027.31 ± 3058.424 to 34730.78 ± 1173.92 by hypothermia treatment in GD-treated groups (F = 75.201. P < 0.001). In addition, as an oxidative stress marker, the heme oxygenase-1 (HO-1) levels were determined with western blot. As shown in Fig. 2c, GD treatment for 16 h caused a significant increase compared to that in normal cultured cells, yet hypothermia treatment remarkably attenuated HO-1 upregulation. Mitochondrial membrane potential was further detected with 5,5′,6,6′-Tetrachloro-1,1′,3,3′-tetraethylbenzimidazolo-carbocyanine iodide (JC-1) staining as a method to evaluate cellar mitochondrial function. Fig. 3a demonstrates that after 16 h GD treatment, the mitochondrial membrane potential exhibited depolarization in the most cells, which were stained with green fluorescence from JC-1; however, hypothermic treatment significantly maintained the polarization of the mitochondrial membrane. Moreover, mitochondrial outer membrane permeabilization (MOMP)-related proteins BAX and Bcl-2 were determined with western blot. Fig. 3c shows that a marked increase of BAX and decline of Bcl-2 were detected in GD-treated cells, while hypothermic treatment significantly reversed the variation tendency. Lastly, the typical apoptotic markers of intrinsic death pathway, cleaved Caspase-3 and 9, were measured. As shown in Fig. 4a, GD treatment caused clear activation of Caspase-3 and 9, which were indicated by an extra cleaved band underneath the main band as detected with western blot, yet the hypothermic culture markedly suppressed the activation of Caspase-3 and 9, showing a significantly reduced active form in both caspases (3 and 9). Taken together, these results suggest that hypothermic treatment maintains mitochondrial function and blocks intrinsic caspase-dependent apoptosis pathways.

3.3. Cirbp plays a key role in hypothermia-induced neuroprotection

To further decipher the molecular mechanism of hypothermia-induced neuroprotection, the role of Cirbp was investigated with gene-modified lentivirus. First, Fig. 5a demonstrates that the level of Cirbp was remarkably upregulated in hypothermia-treated cells, whether cultured with glucose-free medium or not, indicating that Cirbp might be an important factor in hypothermia-induced neuroprotection. Next, green fluorescent protein (GFP)-labeled lentivirus vector and GFP-labeled Cirbp lentivirus vector were constructed and transfected into 661 W cells (Fig. 5c). Overexpression of Cirbp was able to significantly attenuate GD-induced cell death, even under normal cultured conditions (37 °C), decreasing death rate from 83.36 ± 0.87 to 8.47 ± 0.61% when compared to the overexpression of the GFP-alone group detected with PI (Fig. 6b). This suggests that overexpression of Cirbp is able to mimic the hypothermia-induced neuroprotection under normal temperature conditions. Additionally, the influence of over-expressing Cirbp on apoptotic signals was further investigated. As shown in Fig. 6d, overexpressed Cirbp caused a significant decline in BAX and cleaved Caspase 3 under GD conditions, but the expression of Bcl-2 was upregulated. These results demonstrate that Cirbp is a key factor in hypothermia-induced neuroprotection, and over-expressing Cirbp is able to mimic protection similar to hypothermia produces.

3.4. Knocking down Cirbp Compromises the hypothermia-induced neuroprotection

To further confirm the role of Cirbp in hypothermia-induced neuroprotection, the specific shRNA-Cirbp and negative control shRNA were designed and inserted into lentiviral vectors. As shown in Fig. 7a, GD treatment caused massive cell death, as detected with PI staining, while the cells cultured under hypothermic conditions (32 °C) were more resistant to the GD injury, showing reduced cell death percentage. The reason for setting the temperature to be 32 °C as the hypothermic conditions is based on previous studies (Karnatovskaia et al., 2014; Sakurai et al., 2006). However, the cells transfected with negative control shRNA failed to interrupt the neuroprotection produced by hypothermia, yet knocking down Cirbp with specific shRNA almost blocked hypothermia-induced protection in GD-treated cells, showing a cell death percentage similar to cells cultured under normal temperature conditions. Consistently, the knockdown of Cirbp caused the increase of BAX and cleaved Caspase-3, as well as marked decline of Bcl-2 in the further analysis of apoptotic signals. Therefore, these results indicate that Cirbp plays a crucial role in the molecular mechanism of

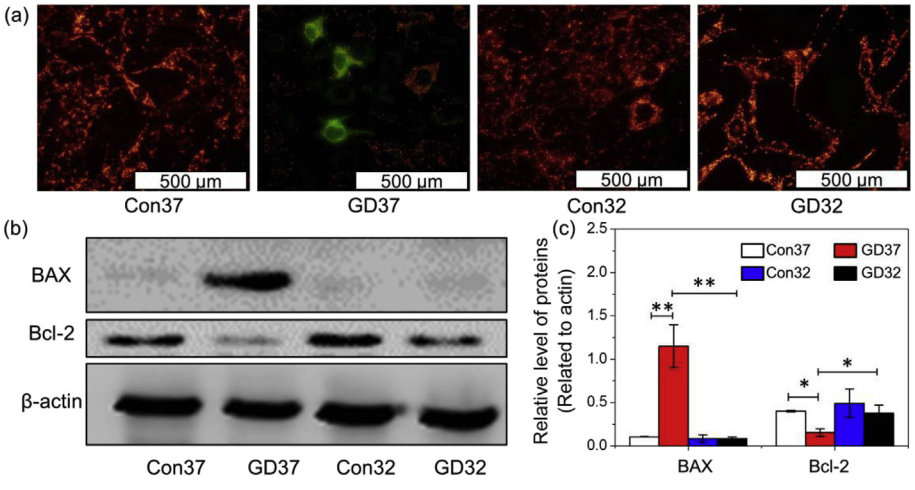

Fig. 3. Hypothermic treatment improves mitochondrial membrane potential. (a) The mitochondrial membrane potential of 661w cells cultured in normal or glucose-free medium for 16 h at 37 °C or 32 °C were analyzed by JC-1 staining under a fluorescence microscope. The mitochondria with normal Δψm were stained with red punctuated fluorescence (JC-1 positive), but mitochondria with depolarized Δψm were stained with green fluorescence. (b) (c) BAX and Bcl-2 were detected by western blot. The molecular weight of BAX, Bcl-2 and β-actin are 21, 26 and 43 kD, respectively. Protein bands on the Western blots were scanned, and the intensity was determined by optical density measurements. F (BAX) = 36.008. P (Con37, GD37; BAX) < 0.001. P (GD37, GD32; BAX) < 0.001. F (Bcl-2) = 6.494. P (Con37, GD37; Bcl-2) = 0.014. P (GD37, GD32; Bcl-2) = 0.023. These results are presented as means ± SEM. (n (number of independent experiments) = 3. ∗: $P < 0.05$, ∗∗: $P < 0.01$).

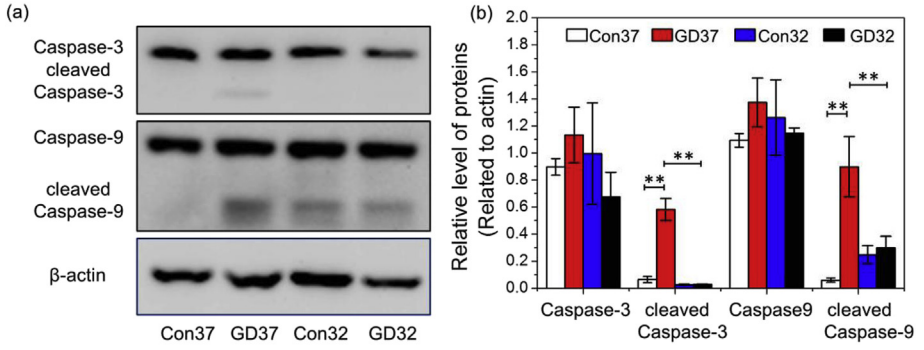

Fig. 4. Hypothermia treatment suppresses caspase-dependent apoptotic pathway. (a) The 661 W cells were cultured in glucose-free medium for 16 h at 37 °C or 32 °C. Caspase-3 and Caspase-9 were detected by western blot. β-actin was used as a loading control protein. (b) Protein bands on the western blots were scanned, and the intensity was determined by optical density measurements. The molecular weight of Caspase-3, cleaved Caspase-3, Caspase-9, cleaved Caspase-9 and β-actin are 35, 19, 49, 39 and 43 kD, respectively. F (cleaved Caspase-3) = 120.808. P (Con37, GD37; cleaved Caspase-3) < 0.001. P (GD37, GD32; cleaved Caspase-3) < 0.001. F (cleaved Caspase-9) = 17.073. P (Con37, GD37; cleaved Caspase-9) < 0.001. P (GD37, GD32; cleaved Caspase-9) = 0.001. These results are presented as means ± SEM. (n (number of independent experiments) = 3. ∗: $P < 0.05$, ∗∗: $P < 0.01$).

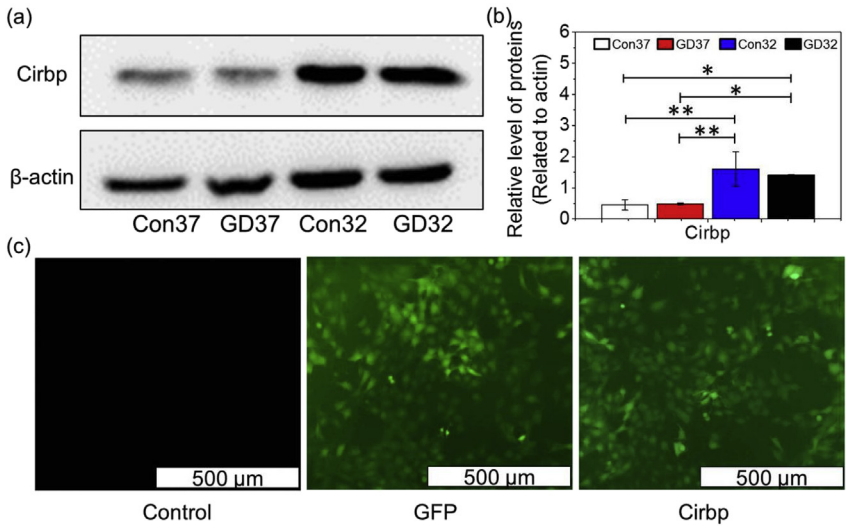

Fig. 5. Cirbp was upregulated under hypothermic conditions. (a) Cirbp was detected by western blot. β-actin was used as a loading control protein. (b) Protein bands on the western blots were scanned, and the intensity was determined by optical density measurements. The molecular weight of Cirbp and β-actin are 19 and 43 kD, respectively. F = 8.727. P (Con37, Con32) = 0.004. P (Con37, GD32) = 0.011. P (GD37, Con32) = 0.005. P (GD37, GD32) < 0.001. (c) 661w cells were transfected by GFP lentivirus and Cirbp lentivirus. These results are presented as means ± SEM. (n (number of independent experiments) = 3. ∗: $P < 0.05$, ∗∗: $P < 0.01$). Control: no vector control, GFP: Lenti-GFP transduction control, Cirbp: Lenti-Cirbp transduction group.

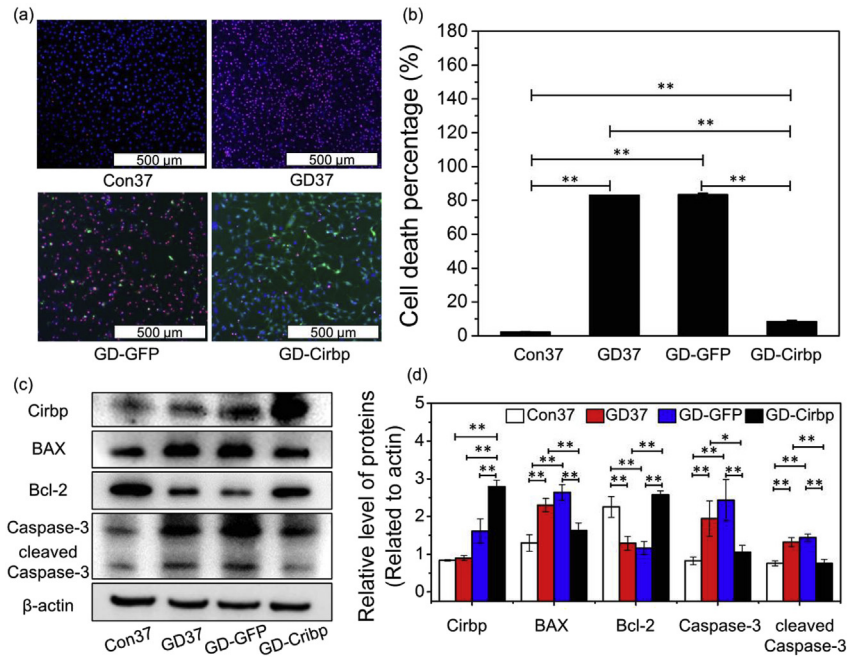

Fig. 6. Effects of overexpressing Cirbp in 661 W cells using Lenti-Cirbp. (a) The 661 W cells, GFP-lentivirus-transfected cells, and Cirbp-lentivirus-transfected cells were cultured in glucose-free medium for 16 h at 37 °C by PI/Hoechst staining. (b) Quantitative assessment of cell death was performed with flow cytometry for PI/Hoechst staining. F = 7549.26. P (Con37, GD37) < 0.001. P (Con37, GD-GFP) < 0.001. P (Con37, GD-Cirbp) < 0.001. P (GD37, GD-Cirbp) < 0.001.P (GD-GFP, GD-Cirbp) < 0.001. (c) Cirbp, BAX, Bcl-2, and Caspase-3 were detected by western blot; β-actin was used as a loading control protein. The molecular weight of Cirbp, BAX, Bcl-2, Caspase-3, cleaved Caspase-3 and β-actin are 19, 21, 26, 35, 19 and 43 kD, respectively. (d) Protein bands on the western blots were scanned, and the intensity was determined by optical density measurements. F (Cirbp) = 72.754. P (Con37, GD-Cirbp; Cirbp) < 0.001. P (GD37, GD-Cirbp; Cirbp) < 0.001. P (GD-GFP, GD-Cirbp; Cirbp) < 0.001. F (BAX) = 18.598. P (Con37, GD37; BAX) = 0.001. P (Con37, GD-GFP; BAX) < 0.001. P (GD37, GD-Cirbp; BAX) < 0.001.P (GD-GFP, GD-Cirbp, BAX) < 0.001. F (Caspase-3) = 12.13. P (Con37, GD37; Caspase-3) = 0.007. P (Con37, GD-GFP; Caspase-3) = 0.001. P (GD37, GD-Cirbp; Caspase-3) = 0.2.P (GD-GFP, GD-Cirbp; Caspase-3) = 0.002. F (cleaved Caspase-3) = 40.628. P (Con37, GD37; cleaved Caspase-3) < 0.001. P (Con37, GD-GFP; cleaved Caspase-3) < 0.001. P (GD37, GD-Cirbp; cleaved Caspase-3) < 0.001.P (GD-GFP, GD-Cirbp; cleaved Caspase-3) < 0.001. These results are presented as means ± SEM. (n (number of independent experiments) = 3. ∗: $P < 0.05$, ∗∗: $P < 0.01$). Con: no vector control, GFP: Lenti-GFP transduction control, Cirbp: Lenti-Cirbp transduction group.

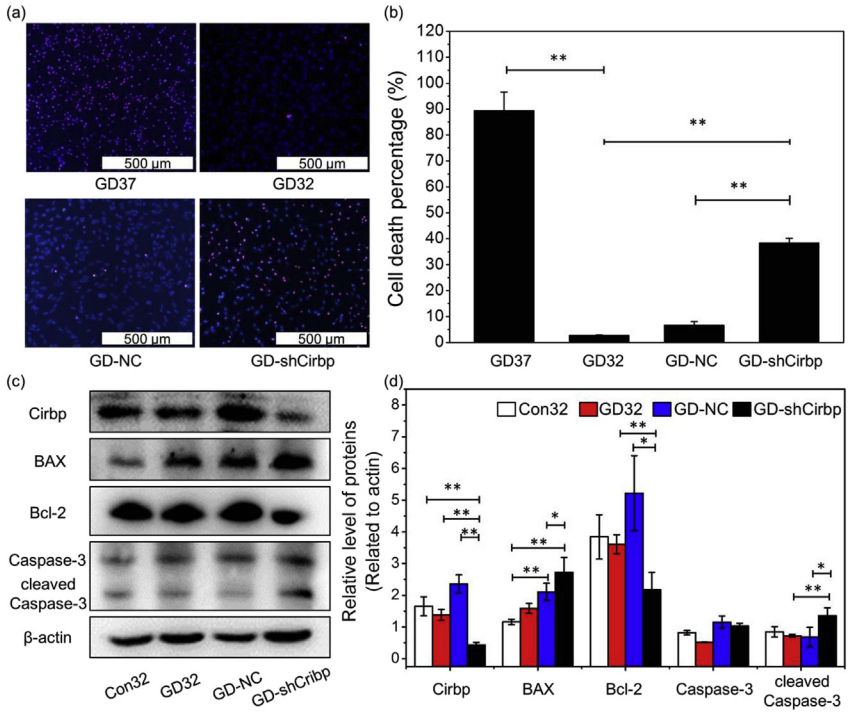

Fig. 7. Effects of knocking down Cirbp on 661 W cells using Lenti-shCirbp. (a) The 661 W cells, negative control lentivirus-transfected cells, and shCirbp-lentivirus-transfected cells were cultured in glucose-free medium for 16 h at 37 °C or 32 °C by PI/Hoechst staining. (b) Quantitative assessment of cell death was performed with flow cytometry for PI/Hoechst staining. F = 326.71. P (GD37, GD32) < 0.001. P (GD32, GD-shCirbp) < 0.001. P (GD-NC, GD-shCirbp) < 0.001. (c) Cirbp, BAX, Bcl-2 and Caspase-3 were detected by western blot. β-actin was used as a loading control protein. The molecular weight of Cirbp, BAX, Bcl-2, Caspase-3, cleaved Caspase-3 and β-actin are 19, 21, 26, 35, 19 and 43 kD, respectively. (d) Protein bands on the western blots were scanned, and the intensity was determined by optical density measurements. F (Cirbp) = 37.055. P (GD37, GD-shCirbp; Cirbp) < 0.001. P (GD32, GD-shCirbp; Cirbp) = 0.001. P (GD-NC, GD-shCirbp; Cirbp) < 0.001. F (BAX) = 17.191. P (GD37, GD-NC, BAX) = 0.003. P (GD37, GD-shCirbp; BAX) < 0.001. P (GD-NC, GD-shCirbp; BAX) = 0.027. F (Bcl-2) = 8.215. P (GD32, GD-shCirbp; Bcl-2) = 0.049. P (GD-NC, GD-shCirbp; Bcl-2) = 0.001. F (cleaved Caspase-3) = 4.279. P (GD32, GD-shCirbp; cleaved Caspase-3) = 0.017. P (GD-NC, GD-shCirbp; cleaved Caspase-3) = 0.013. These results are presented as means ± SEM. (n (number of independent experiments) = 3. ∗: $P < 0.05$, ∗∗: $P < 0.01$). Con: no vector control, NC: negative control lentivirus transduction control, shCirbp: Lenti-Cirbp transduction group.

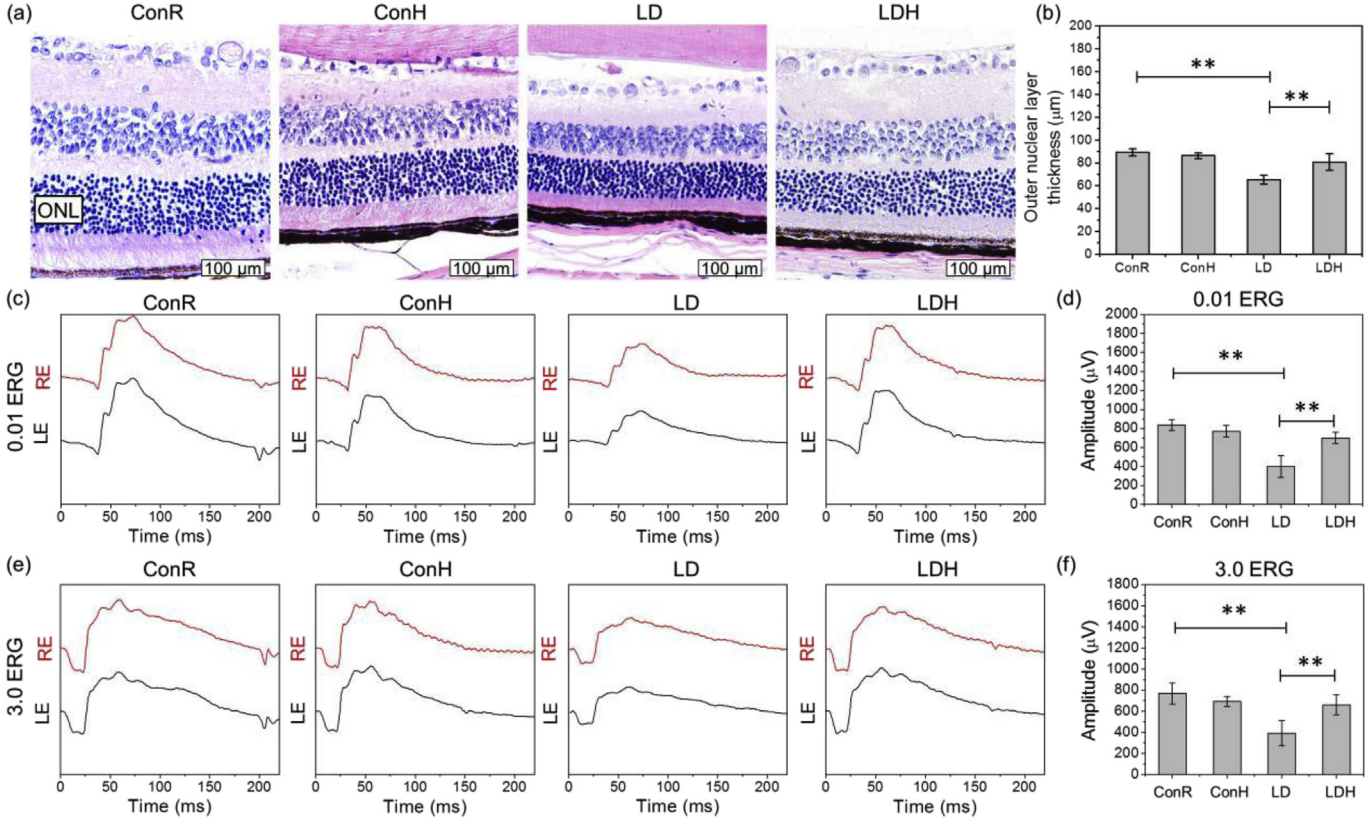

Fig. 8. Hypothermia treatment suppresses light damage on retina *in vivo*. Mice were given hypothermic treatment with or without light exposure. (a) (b) The thickness of the outer nuclear segment was measured after HE staining in retinal slices. F = 21.599. P (ConR, LD) < 0.001. P (LD, LDH) < 0.001. (c)–(f) ERG was used to evaluate the retinal function. The dark-adapted (scotopic 0.01, b-wave) and light-adapted (photopic 3.0, a-wave) ERGs were recorded. F (0.01 ERG) = 24.606. P (ConR, LD; 0.01 ERG) < 0.001. P (LD, LDH; 0.01 ERG) < 0.001. F (3.0 ERG) = 12.073. P (ConR, LD; 3.0 ERG) < 0.001. P (LD, LDH; 3.0 ERG) = 0.001. Data are shown as means ± SEM. (n (number of animals) = 5. ∗: $P < 0.05$, ∗∗: $P < 0.01$). ConR: control group, ConH: hypothermia control group, LD: light damage group, LDH: light damage and hypothermia group.

hypothermia-induced neuroprotection.

3.5. Therapeutic hypothermia protects the retina against light injury

To further verify the hypothermia-induced protection in retina neurons, a light-injured mice model was constructed. As shown in Fig. 8c, hypothermic treatment had no influence on retina function without statistical significance in a-wave (3.0 electroretinogram (ERG)) and b-wave (0.01 ERG) values as evaluated with ERG when compared to those mice fed under normal temperature conditions. However, the 12 h exposure of 7500 Lux visible light led to severe damage in retinal function, showing remarkable decline in a-wave (3.0 ERG) and b-wave (0.01 ERG) values as compared to mice in the normal control group. The hypothermic treatment produced obvious protection against light injury, increasing a-wave value from 369.38 ± 127.56 to 631.74 ± 126.80 and b-wave value from 388.93 ± 138.93 to 660.12 ± 113.96 (F (0.01 ERG) = 24.606. P (LD, LDH; 0.01 ERG) < 0.001. F (3.0 ERG) = 12.073. P (LD, LDH; 3.0 ERG) = 0.001). Additionally, the thickness of the outer nuclear segment was measured after hematoxylin-eosin (HE) staining in retinal slices. Similarly, Fig. 8b shows that there was no statistical difference in outer nuclear layer (ONL) thickness between the hypothermia-treated group and normal control group, yet light exposure caused marked thickening in ONL, reducing the thickness from 89.16 ± 3.09 to 65.29 ± 3.90 μm (F = 21.599. P < 0.001). In addition, the thickness of the inner plexiform layer, inner nuclear layer, and outer segment were also evaluated, indicating similar tendencies (Fig. S1). However, the hypothermic treatment maintained the thickness of ONL with a statistical significance even after light exposure. The further biochemical analysis of retina tissue demonstrated that Cirbp was remarkably upregulated under hypothermic conditions and reduced by light exposure. Compared with the light exposure group, Cirbp was upregulated in the hypothermia-treated light exposure group. Since poly(ADP-ribose) polymerase-1 (PARP-1) is a key marker evaluating light-induced cell death in the retina, the level of PARP-1 was determined with western blot. Fig. 9 shows that light exposure led to marked upregulation of PARP-1 (89 kDa), while an obvious decline was detected in hypothermia-treated mice retinas. In total, these results suggest that therapeutic hypothermia protects the retina against light injury.

4. Discussion

Glucose deprivation mimics acute energy depletion, which is one of the critical factors contributing to the pathogenic mechanisms of retinal ischemia. When glucose is not enough, mitochondria cannot produce enough energy for cells, and a caspase-dependent death and oxidative stress injury are induced. These results demonstrate that oxidative stress and caspase-dependent apoptosis were activated in photoreceptors at 16 h after GD, which produced massive intracellular ROS detected by the DCFH-DA assay and activated apoptosis relative protein detected by western blotting. Some factors were involved in the death cascade. HO-1 is an endogenous antioxidant defense component that is upregulated during oxidative stress (Chandra et al., 2000). The results presented here showed that the level of HO-1 was increased significantly in photoreceptors after 16 h of GD injury. In addition, GD-induced oxidative stress activated the intrinsic caspase-dependent apoptotic pathways, yet the intrinsic apoptotic pathway is considered closely regulated by MOMP (Kalkavan and Green, 2018). Bcl-2 family proteins play a key role in the intrinsic caspase-dependent apoptosis, as they are widely involved in modulating MOMP. The correct targeting of the Bcl-2 family to mitochondria is also critical for initiating the apoptotic cascade. The formation of pores in the outer mitochondrial membrane (OMM) is achieved by the integration and conformational change of activated BAX and Bcl-2 homologous antagonist killer (BAK). To trigger MOMP, BAX is translocated to the OMM, and BAK is disengaged from anti-apoptotic Bcl-2 proteins. These results show that the anti-apoptotic factor Bcl-2 was decreased in photoreceptors after 16 h of GD injury, while the pro-apoptotic protein BAX was increased, as detected in the western blot. Meanwhile, the dysfunction of the mitochondria was also verified by measuring mitochondrial membrane potential with JC-1, which showed a marked number of cells losing functional Δψm after 16 h GD injury. Furthermore, the marker proteins of intrinsic apoptosis, Caspase-3 and Caspase-9, were activated, and the cleaved forms of the proteins were markedly upregulated after 16 h of injury.

Excessive light exposure has been considered a toxic factor for retina degeneration, although the eye has its own mechanisms to protect the retina from visible light during biological evolution (Youssef et al., 2011). It has been revealed that the most severe damage caused by light exposure is normally located at photoreceptor cells (Organisciak and Vaughan, 2010). Unlike GD-induced cell death by caspase-dependent pathways, light exposure induced a caspase-independent mechanism called parthanatos. Previous researches have proven that parthanatos does not require caspases but is dependent on the PARP-1-mediated accumulation of PAR (poly ADP-ribose) and the subsequent nuclear translocation of the apoptosis-inducing factor (AIF) (Liu et al., 2018). PARP-1 is a well-conserved nuclear enzyme that repairs DNA damage and is extremely sensitive to various DNA lesions (Dawson and Dawson, 2004; Osborne et al., 2010; Van Wijk and Hageman, 2005). Light exposure may cause excessive generation of ROS in retinas via photooxidation injury (Osborne et al., 2010). ROS is able to penetrate nuclear membranes and further cause DNA breaks, which activates PARP-1 to repair the DNA damage. However, excessive activation of PARP-1 triggers the PARP-dependent death pathway. Therefore, PARP-1 is a marker in light-induced damage. In this study, PARP-1 exhibited remarkable upregulation in light-injured retinas. The presented results demonstrated that hypothermia treatment increased the expression of Cirbp and decreased the expression of PARP-1 in light-injured retinas,

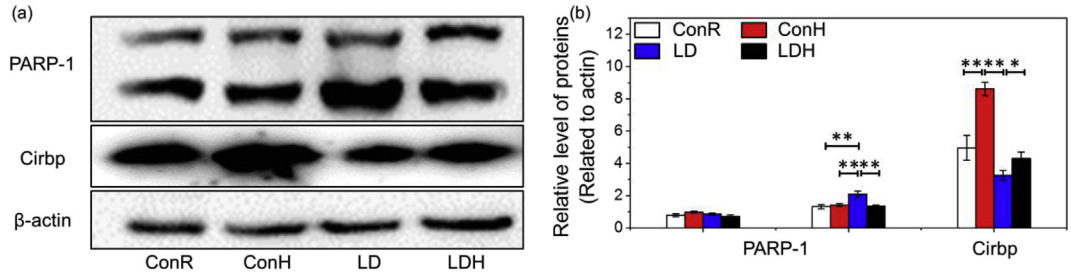

Fig. 9. Hypothermia treatment suppresses PARP-dependent apoptotic pathway. (a) PARP-1 and Cirbp were detected by western blot. β-actin was used as a loading control protein. The molecular weight of PARP-1, Cirbp and β-actin are 116, 89, 19 and 43 kD, respectively. (b) Protein bands on the western blots were scanned, and the intensity was determined by optical density measurements. F (PARP-1) = 26.501. P (ConR, LD; PARP-1) < 0.001. P (ConH, LD; PARP-1) < 0.001. P (LD, LDH; PARP-1) < 0.001. F (Cirbp) = 64.5. P (ConR, LD; Cirbp) < 0.001. P (ConH, LD; Cirbp) < 0.001. P (LD, LDH) = 0.033. These results are presented as means ± SEM. (n (number of independent experiments) = 3. ∗: P < 0.05, ∗∗: P < 0.01).

indicating that the activation of Cirbp induced by hypothermia may suppress PARP-dependent neuron death in retinas from light-induced damage. In addition, the results from *in vivo* experiments demonstrated that the thickness of the ONL was significantly reduced after light exposure. Further ERG evaluation for retinal function also disclosed that the amplitude of a and b-waves was markedly decreased after light exposure. However, 3 h hypothermia treatment was able to maintain thickness of the ONL and increase the value of a and b-waves. Previous studies reveal that hypothermia protects the retina from ischemic damage, improving retinal function and restoring histological changes (Rey-Funes et al., 2017; Salido et al., 2013).

The neuroprotection of hypothermia has been proven in various diseases, including cardiac arrest (Dzieciol et al., 2014), stroke, and traumatic brain injury (Karnatovskaia et al., 2014). Sakurai et al. (Sakurai et al., 2006)reported that hypothermia protected cells from TNF-alpha-induced apoptosis by upregulating extracellular signal-regulated kinase (ERK) and nuclear factor kappa B (NF-κB) pathways, and Li et al. found that hypothermia was able to inhibit H_2O_2-induced apoptosis by inducting TRX and inhibiting Caspase-3 (Li et al., 2012). Consistent with these previous studies, the neuroprotection of hypothermia was verified in photoreceptors against GD-induced injury. The key molecular target in the neuroprotective mechanism was identified as Cirbp. Cirbp, as an RNA-binding factor, composes an RRM and a C-terminal region containing several repeats of the RGG motif (De Leeuw et al., 2007; Liu et al., 2015; Wellmann et al., 2004), which plays an important role in regulating cellular response for cellular stresses caused by hypoxia, ultraviolet light, and hypothermia (Ichinose et al., 2014; Liao et al., 2017). Xia et al. revealed that overexpression of Cirbp was able to upregulate Bcl-2 in BALB/c mouse testicles (Xia et al., 2013). Sakurai et al. found that Cirbp expression increased in the mouse fibroblast cell line BALB/3T3 under hypothermic conditions and inhibited apoptosis induced by TNF-α (Sakurai et al., 2006). Zhang et al. demonstrated that caspase-dependent apoptosis was inhibited in the rat brain cortex neurons by upregulating Cirbp (Zhang et al., 2015). Liu et al. found that recombinant Cirbp showed protection in N2a cells from H_2O_2-induced apoptosis (Liu et al., 2015). In addition, knocking down Cirbp with shRNA-Cirbp blocked neuroprotection under hypothermic conditions in H_2O_2-induced apoptosis and caspase-dependent neuron apoptosis (Li et al., 2012; Zhang et al., 2015), which is consistent with the results presented here. In this study, the overexpression of Cirbp by using gene-modified lentivirus was neuroprotective in photoreceptors, even under normal temperature conditions, blocking the GD-induced, caspase-dependent cell death cascade and light-induced, PARP-dependent parthanatos (Fig. S2). However, knocking down Cirbp with shRNA-integrated lentivirus completely blocked hypothermia-induced neuroprotection.

The cellular mechanisms of retinal damage induced by glucose deprivation or by the exposure to visible light are different. GD induced a caspase-dependent pathway and light exposure induced a caspase-independent pathway, which is a PARP-dependent pathway. However, in this study, we already demonstrated that overexpression of Cirbp was neuroprotective in both GD-induced cell death and light-induced cell death. Overall, these results suggest that Cirbp may function at the upstream signal of both caspase-dependent and PARP-dependent pathways. The possible mechanism of Cirbp protection may inhibit oxidative stress (Scheme 1). Evidence from earlier studies suggests GD induced oxidative stress by generating ROS of the nicotinamide adenine dinucleotide phosphate oxidase (Nox) family enzymes (Bhatt et al., 2010; Kowluru and Kowluru, 2014). Also, the inducible generator of ROS in light-induced oxidative stress is lipofuscin, which is a byproduct of the phagocytosis of outer segments of lipid-rich photoreceptors (Boulton et al., 2004; Chen et al., 2017; Zhao et al., 2014).

In our current research, overexpression Cirbp inhibited ROS production in both GD-induced cell and light-induced cell death (Fig. S3). HO-1 expression detected by western blot was similar in both GD-induced and light-induced cells (Fig. S4). Furthermore, Cirbp may inhibit

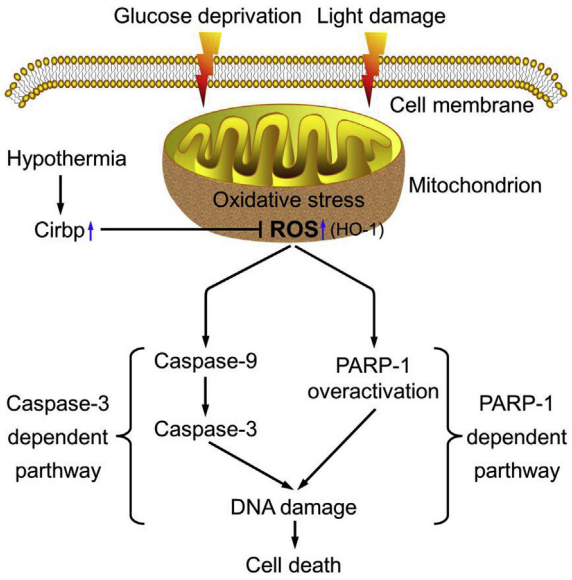

Scheme 1. A schematic diagram of the mechanism of hypothermia protective effect.

ROS production by activating TRX. TRX is a well-known ROS scavenger (Park et al., 1999; Welsh et al., 2002). Yokomizo et al. demonstrated that Cirbp bound specifically to the 3' UTR of TRX mRNA, which enhanced TRX expression (Yokomizo et al., 1995). Since ROS plays a crucial role in both GD-induced and light-induced cell death, Cirbp exhibits neuroprotection from both. Then, Cirbp may suppress cell death mainly through functioning TRX, but the detailed molecular mechanism requires further investigation.

5. Summary

Hypothermia shows marked neuroprotection in photoreceptors against GD injury, as well as against light injury. Hypothermia suppressed massive generation of cellular ROS, blocked caspase-dependent apoptosis in GD-injured photoreceptors, and inhibited the activation of PARP-1 in light-damaged retinas. Importantly, Cirbp was verified as a key molecular target in hypothermia-induced neuroprotection. Overexpressing or knocking-down Cirbp markedly regulated hypothermia-caused neuroprotection. Cirbp may function at the upstream signal of both caspase-dependent and PARP-dependent pathways. The possible mechanism of Cirbp protection may inhibit oxidative stress. However, Cirbp protection needs further experimentation *in vivo* either by overexpressing or knocking-down Cirbp in animals. These findings may provide a potential approach for treating retinal degeneration diseases and retina ischemia.

Disclosure

The authors declare no competing financial interest.

Acknowledgments

This research was funded by grants from the National Natural Science Foundation of China (No: 81570864), and the Natural Science Foundation of Jilin Province (No: 20160101004JC, No: 20160414045GH). We thank Dr. Muayyad Al-Ubaidi, Department of Cell Biology, University of Oklahoma Health Sciences Center, Oklahoma City, OK, USA for 661 W cell line.

Appendix A. Supplementary data

Supplementary data to this article can be found online at https://doi.org/10.1016/j.neuint.2019.03.006.

References

Bhatt, L., Groeger, G., McDermott, K., Cotter, T.G., 2010. Rod and cone photoreceptor cells produce ROS in response to stress in a live retinal explant system. Mol. Vis. 16, 283–293.

Boulton, M., Rózanowska, M., Rózanowski, B., Wess, T., 2004. The photoreactivity of ocular lipofuscin. Photochem. Photobiol. Sci. 3, 759–764.

Cattaneo, G., Schumacher, M., Maurer, C., Wolfertz, J., Jost, T., Büchert, M., Keuler, A., Boos, L., Shah, M.J., Foerster, K., Niesen, W.D., Ihorst, G., Urbach, H., Meckel, S., 2016. Endovascular cooling catheter for selective brain hypothermia: an animal feasibility study of cooling performance. AJNR Am. J. Neuroradiol. 37, 885–891.

Chandra, J., Samali, A., Orrenius, S., 2000. Triggering and modulation of apoptosis by oxidative stress. Free Radical Biol. Med. 29, 323–333.

Chao, H.M., Chen, I.L., Liu, J.H., 2014. S-allyl L-cysteine protects the retina against kainate excitotoxicity in the rat. Am. J. Chin. Med. 42, 693–708.

Chen, W.J., Wu, C., Xu, Z.J., Kuse, Y., Hara, H., Duh, E.J., 2017. Nrf2 protects photoreceptor cells from photo-oxidative stress induced by blue light. Exp. Eye Res. 154, 151–158.

Dawson, V.L., Dawson, T.M., 2004. Deadly conversations: nuclear-mitochondrial cross-talk. J. Bioenerg. Biomembr. 36, 287–294.

De Leeuw, F., Zhang, T., Wauquier, C., Huez, G., Kruys, V., Gueydan, C., 2007. The cold-inducible RNA-binding protein migrates from the nucleus to cytoplasmic stress granules by a methylation-dependent mechanism and acts as a translational repressor. Exp. Cell Res. 313, 4130–4144.

Dell'Anna, A.M., Taccone, F.S., Halenarova, K., Citerio, G., 2014. Sedation after cardiac arrest and during therapeutic hypothermia. Minerva Anestesiol. 80, 954–962.

Demirgan, S., Erkalp, K., Sevdi, M.S., Aydogmus, M.T., Kutbay, N., Firincioglu, A., Ozalp, A., Alagol, A., 2014. Cardiac condition during cooling and rewarming periods of therapeutic hypothermia after cardiopulmonary resuscitation. BMC Anesthesiol. 14, 78.

Dzieciol, M., Kacprzak, M., Goleniewska, B., Zielińska, M., 2014. Osborn wave in patients with ST-elevation myocardial infarction undergoing mild therapeutic hypothermia after cardiac arrest. Acta Cardiol. 69, 532–540.

Fan, B., Wang, B.F., Che, L., Sun, Y.J., Liu, S.Y., Li, G.Y., 2017. Blockage of NOX2/MAPK/NF-κB pathway protects photoreceptors against glucose deprivation-induced cell death. Oxid. Med. Cell. Longevity 2017, 5093473.

Ichinose, M., Kamei, Y., Iriyama, T., Imada, S., Seyama, T., Toshimitsu, M., Asou, H., Yamamoto, M., Fujii, T., 2014. Hypothermia attenuates apoptosis and protects contact between myelin basic protein-expressing oligodendroglial-lineage cells and neurons against hypoxia-ischemia. J. Neurosci. Res. 92, 1270–1285.

Iftode, C., Daniely, Y., Borowiec, J.A., 1999. Replication protein a (RPA): the eukaryotic SSB. Crit. Rev. Biochem. Mol. Biol. 34, 141–180.

Kalkavan, H., Green, D.R., 2018. MOMP, cell suicide as a BCL-2 family business. Cell Death Differ. 25, 46–55.

Karnatovskaia, L.V., Wartenberg, K.E., Freeman, W.D., 2014. Therapeutic hypothermia for neuroprotection: history, mechanisms, risks, and clinical applications. Neurohospitalist 4, 153–163.

Kim, J.Y., Kim, N., Yenari, M.A., Chang, W.H., 2013. Hypothermia and pharmacological regimens that prevent overexpression and overactivity of the extracellular calcium-sensing receptor protect neurons against traumatic brain injury. J. Neurotrauma 30, 1170–1176.

Kowluru, A., Kowluru, R.A., 2014. Phagocyte-like NADPH oxidase [Nox2] in cellular dysfunction in models of glucolipotoxicity and diabetes. Biochem. Pharmacol. 88, 275–283.

Li, S.C., Zhang, Z.W., Xue, J.H., Liu, A.J., Zhang, H.T., 2012. Cold-inducible RNA binding protein inhibits H_2O_2-induced apoptosis in rat cortical neurons. Brain Res. 1441, 47–52.

Liao, Y., Feng, J.G., Zhang, Y., Tang, L.L., Wu, S.Y., 2017. The mechanism of CIRP in inhibition of keratinocytes growth arrest and apoptosis following low dose UVB radiation. Mol. Carcinog. 56, 1554–1569.

Liu, J.L., Xue, J.H., Zhang, H.T., Li, S.C., Liu, Y.X., Xu, D.G., Zou, M.J., Zhang, Z.W., Diao, J.F., 2015. Cloning, expression, and purification of cold inducible RNA-binding protein and its neuroprotective mechanism of action. Brain Res. 1597, 189–195.

Liu, S.Y., Song, J.Y., Fan, B., Wang, Y., Pan, Y.R., Che, L., Sun, Y.J., Li, G.Y., 2018. Resveratrol protects photoreceptors by blocking caspase- and PARP-dependent cell death pathways. Free Radical Biol. Med. 129, 569–581.

Mori, K., Yoneya, S., Hayashi, N., Abe, T., 1997. Fundus hypothermia inhibits retinal damage induced by visible blue light. Nippon. Ganka Gakkai Zasshi 101, 633–638.

Organisciak, D.T., Vaughan, D.K., 2010. Retinal light damage: mechanisms and protection. Prog. Retin. Eye Res. 29, 113–134.

Osborne, N.N., Casson, R.J., Wood, J.P.M., Chidlow, G., Graham, M., Melena, J., 2004. Retinal ischemia: mechanisms of damage and potential therapeutic strategies. Prog. Retin. Eye Res. 23, 91–147.

Osborne, N.N., Li, G.Y., Ji, D., Mortiboys, H.J., Jackson, S., 2010. Light affects mitochondria to cause apoptosis to cultured cells: possible relevance to ganglion cell death in certain optic neuropathies. J. Neurochem. 105, 2013–2028.

Park, J.S., Park, S.J., Peng, X.D., Wang, M., Yu, M.A., Lee, S.H., 1999. Involvement of DNA-dependent protein kinase in UV-induced replication arrest. J. Biol. Chem. 274, 32520–32527.

Peng, P.H., Chao, H.M., Juan, S.H., Chen, C.F., Liu, J.H., Ko, M.L., 2011. Pharmacological preconditioning by low dose cobalt protoporphyrin induces heme oxygenase-1 overexpression and alleviates retinal ischemia-reperfusion injury in rats. Curr. Eye Res. 36, 238–246.

Reinhard, K., Mutter, M., Gustafsson, E., Gustafsson, L., Vaegler, M., Schultheiss, M., Müller, S., Yoeruek, E., Schrader, M., Münch, T.A., 2016. Hypothermia promotes survival of ischemic retinal ganglion cells. Investig. Ophthalmol. Vis. Sci. 57, 658–663.

Rey-Funes, M., Larrayoz, I.M., Contartese, D.S., Soliño, M., Sarotto, A., Bustelo, M., Bruno, M., Dorfman, V.B., Loidl, C.F., Martínez, A., 2017. Hypothermia prevents retinal damage generated by optic nerve trauma in the rat. Sci. Rep. 7, 6966.

Sahara, T., Goda, T., Ohgiya, S., 2002. Comprehensive expression analysis of time-dependent genetic responses in yeast cells to low temperature. J. Biol. Chem. 277, 50015–50021.

Sakurai, T., Itoh, K., Higashitsuji, H., Nonoguchi, K., Liu, Y., Watanabe, H., Nakano, T., Fukumoto, M., Chiba, T., Fujita, J., 2006. Cirp protects against tumor necrosis factor-α-induced apoptosis via activation of extracellular signal-regulated kinase. Biochim. Biophys. Acta 1763, 290–295.

Salido, E.M., Dorfman, D., Bordone, M., Chianelli, M., González Fleitas, M.F., Rosenstein, R.E., 2013. Global and ocular hypothermic preconditioning protect the rat retina from ischemic damage. PLoS One 8, e61656.

Van Wijk, S.J.L., Hageman, G.J., 2005. Poly(ADP-ribose) polymerase-1 mediated caspase-independent cell death after ischemia/reperfusion. Free Radical Biol. Med. 39, 81–90.

Wang, H.Y., Cui, X.F., Gu, Q., Chen, Y., Zhou, J., Kuang, Y., Wang, Z.A., Xu, X., 2012. Retinol dehydrogenase 13 protects the mouse retina from acute light damage. Mol. Vis. 18, 1021–1030.

Wellmann, S., Bührer, C., Moderegger, E., Zelmer, A., Kirschner, R., Koehne, P., Fujita, J., Seeger, K., 2004. Oxygen-regulated expression of the RNA-binding proteins RBM3 and CIRP by a HIF-1-Independent mechanism. J. Cell Sci. 117, 1785–1794.

Welsh, S.J., Bellamy, W.T., Briehl, M.M., Powis, G., 2002. The redox protein thioredoxin-1 (Trx-1) increases hypoxia-inducible factor 1α protein expression: trx-1 overexpression results in increased vascular endothelial growth factor production and enhanced tumor angiogenesis. Cancer Res. 62, 5089–5095.

Wenzel, A., Grimm, C., Samardzija, M., Remé, C.E., 2005. Molecular mechanisms of light-induced photoreceptor apoptosis and neuroprotection for retinal degeneration. Prog. Retin. Eye Res. 24, 275–306.

Winkler, B.S., 1981. Glycolytic and oxidative metabolism in relation to retinal function. J. Gen. Physiol. 77, 667–692.

Wu, L., Sun, H.L., Gao, Y., Hui, K.L., Xu, M.M., Zhong, H., Duan, M.L., 2017. Therapeutic hypothermia enhances cold-inducible RNA-binding protein expression and inhibits mitochondrial apoptosis in a rat model of cardiac arrest. Mol. Neurobiol. 54, 2697–2705.

Xia, Z., Jiang, K., Liu, T., Zheng, H., Liu, X., Zheng, X., 2013. The protective effect of cold-inducible RNA-binding protein (CIRP) on testicular torsion/detorsion: an experimental study in mice. J. Pediatr. Surg. 48, 2140–2147.

Xu, W.S., Ngo, L., Perez, G., Dokmanovic, M., Marks, P.A., 2006. Intrinsic apoptotic and thioredoxin pathways in human prostate cancer cell response to histone deacetylase inhibitor. Proc. Natl. Acad. Sci. U. S. A 103, 15540–15545.

Yokomizo, A., Ono, M., Nanri, H., Makino, Y., Ohga, T., Wada, M., Okamoto, T., Yodoi, J., Kuwano, M., Kohno, K., 1995. Cellular levels of thioredoxin associated with drug sensitivity to cisplatin, mitomycin C, doxorubicin, and etoposide. Cancer Res. 55, 4293–4296.

Youssef, P.N., Sheibani, N., Albert, D.M., 2011. Retinal light toxicity. Eye 25, 1–14.

Zhang, H.T., Xue, J.H., Zhang, Z.W., Kong, H.B., Liu, A.J., Li, S.C., Xu, D.G., 2015. Cold-inducible RNA-binding protein inhibits neuron apoptosis through the suppression of mitochondrial apoptosis. Brain Res. 1622, 474–483.

Zhao, Z., Sun, T., Jiang, Y., Wu, L.J., Cai, X.Z., Sun, X.D., Sun, X.J., 2014. Photooxidative damage in retinal pigment epithelial cells via GRP78 and the protective role of grape skin polyphenols. Food Chem. Toxicol. 74, 216–224.

Zhou, T., Liang, L., Liang, Y., Yu, T., Zeng, C., Jiang, L., 2017. Mild hypothermia protects hippocampal neurons against oxygen-glucose deprivation/reperfusion-induced injury by improving lysosomal function and autophagic flux. Exp. Cell Res. 358, 147–160.

Zhu, X.Z., Bührer, C., Wellmann, S., 2016. Cold-inducible proteins CIRP and RBM3, a unique couple with activities far beyond the cold. Cell. Mol. Life Sci. 73, 3839–3859.